

# Order parameter by instantaneous normal mode analysis for melting behaviour of cluster $\text{Ag}_{17}\text{Cu}_2$

Pin-Han Tang<sup>1</sup>, Ten-Ming Wu<sup>1</sup> and S K Lai<sup>2</sup>

<sup>1</sup>Institute of Physics, National Chiao-Tung University, Hsinchu 300, Taiwan

<sup>2</sup>Complex Liquid Laboratory, Department of Physics, National Central University, Chungli 320, Taiwan

Email: tmw@faculty.nctu.edu.tw; sklai@coll.phy.ncu.edu.tw

**Abstract.** We perform isothermal Brownian-type molecular dynamics simulations with the Gupta potential for bimetallic cluster  $\text{Ag}_{17}\text{Cu}_2$  from  $T=0$  to 1500K, across the temperature range associated with the melting behaviour determined by the specific heat of the cluster. We also use the instantaneous normal mode (INM) analysis to dissect dynamics of the cluster. In terms of the projected density of states of the vibrational INMs, we propose a new order parameter that specifically describes the melting behaviour of the cluster. The calculated result of our order parameter is consistent with the information inferred from the specific heat data.

## 1. Introduction

Melting of clusters, which is associated with a transition from the solid-like to the liquid-like cluster structures, is more complicated than that of bulk systems [1]. Due to the finite sizes of clusters, the melting transition of a cluster occurs over a temperature range, rather than at a well-defined temperature [2,3,4]. Instead of a discontinuous jump as in the specific heat of a bulk system at the melting temperature, the specific heat  $C_V$  of a cluster changes continuously with temperature and generally exhibits a single broader peak or a main peak with a prepeak at a lower temperature [3,4,5]; the melting temperature  $T_m$  is usually defined as the temperature at the single peak or the main peak.

Physically, the melting phenomena are described by some appropriated chosen order parameters. The melting of bulk systems at a given pressure is a first-order transition in thermodynamics and commonly characterized by a discontinuous jump in the order parameter, such as entropy or volume, at the melting temperature. For clusters, other order parameters have been used to characterize the transition between the solid-like and liquid-like cluster structures [2]. Theoretically, the bimodality in the probability distribution of the short-time averaged temperature in microcanonical ensemble provides an evidence for the coexistence of the solid-like and liquid-like cluster isomers within a temperature range [6]. By the microcanonical ensemble simulations, the solid-like and liquid-like isomers of a cluster are found to be separated by a barrier in Landau free energy and, therefore, potential energy serves as the order parameter of the free energy [7]. Also based on the short-time average, some geometric order parameters are used to address the transition between two stable isomers and their coexistence [8]. Continuously used in computer simulations [5,9,10], the root-mean-square bond length fluctuation constant  $\delta$  acts as a Lindemann-like order parameter, which signals some kinds of structural or phase transformation. However, the information of the transition deduced from  $\delta$  and  $C_V$  is not always consistent. Recently, by analyzing the cluster dynamics of  $\text{Ag}_{17}\text{Cu}_2$  with



the instantaneous normal mode (INM) theory, we propose a new order parameter, which describes the melting behavior of the cluster in consistence with the information inferred from its specific heat [11]. The main purpose of this proceeding is to address this new order parameter.

## 2. Instantaneous Normal Mode Theory for Clusters

Originally developed for studying the short-time dynamics of liquids from the viewpoint of potential energy landscape [12,13], the INM theory has been a useful analytic tool for investigating microscopic dynamics in condensed matter and fruitful results of bulk systems have been presented. A recent review of the INM theory is given in Ref. [14]. Before applied for bulk systems, the INM analysis has been used to study cluster dynamics in a series of papers in 1990 [15,16,17]. Despite some insight provided by those studies, the strategy to exploit the cluster dynamics with the INM analysis still demands further exploration. The major impediment lies in the particle number. Even for a cluster containing particles less than a hundred, the potential energy landscape of the cluster is extremely complicated in a multi-dimensional space. Differing from the particle motions in bulk systems, whose particle numbers are infinite, a cluster with finite particle number has rotational motions of a whole about its principal axes. This feature causes the INM analysis for clusters in some aspects different from that for bulk systems and results in a new order parameter to monitor the melting behavior of the cluster.

The INMs of a cluster configuration are referred to as the eigenmodes of the Hessian matrix evaluated at the configuration, where the Hessian matrix is defined as the second derivatives of the potential energy function with respect to particle displacements [18]. For a cluster of  $N$  particles with mass  $m_j$ , for  $j=1, \dots, N$ , which may be of different species, the  $3N$  INMs generally contain three translational ( $T_x, T_y, T_z$ ), three rotational ( $R_x, R_y$  and  $R_z$ ) and  $3N-6$  vibrational ( $V_1, \dots, V_{3N-6}$ ) modes. The normalized eigenvector of an INM, indexed with  $\alpha$ , is denoted as  $\vec{e}_j^\alpha$ , where  $\vec{e}_j^\alpha \equiv (e_{jx}^\alpha, e_{jy}^\alpha, e_{jz}^\alpha)$  is the three-dimensional displacement of particle  $j$  in this INM.

The three translational INMs are easily identified with zero eigenvalues. Because of the vibrational-rotational couplings, the three rotational modes of a cluster can be separated out from the rest of vibrational modes by two methods. As the vibrational-rotational couplings are extremely weak, the clusters are close to rigid so that the rotational and vibrational degrees of freedom are assumed to be decoupled and three purely rotational modes of the cluster can be separated out by the standard projection technique [19], which is referred to *Method I* in this proceeding. On the other hand, as the vibrational-rotational couplings are significant, the rotational and vibrational degrees of freedom of a cluster mix to some extent so that the purely rotational modes are not well defined. However, under the INM approximation, a cluster at an instant is considered as a rigid body with the instantaneous structure and its instantaneous total angular momentum is regarded as a constant. Thus, by an alternative method [11,17], which is referred as *Method II*, the approximated rotational modes of a cluster are identified as the INMs that have the three largest angular momenta, whose magnitudes are evaluated by the following formula

$$L_\alpha = c \left| \sum_{j=1}^N \sqrt{m_j} (\vec{r}_j \times \vec{e}_j^\alpha) \right|$$

where  $\vec{r}_j$  is the position of particle  $j$  and  $c$  is the proportionality constant between the instantaneous particle velocity and the normalized INM eigenvector. Note that the constant  $c$  given here is different from the one given in Ref. [17], in which the particles of a cluster are of the same species.

After excluding the translational and rotational modes, the remaining  $3N-6$  INMs of a cluster behave vibrationally and are indexed with the INM frequencies  $\omega_\alpha$ , which are the square roots of the INM eigenvalues. The normalized vibrational density of states (DOS) of a cluster is expressed as

$$D_{vib}(\omega) = \frac{1}{3N-6} \left\langle \sum_{\alpha=1}^{3N-6} \delta(\omega - \omega_\alpha) \right\rangle$$

where the brackets denote an ensemble average over cluster configurations. Generally,  $D_{vib}(\omega)$  consists of two lobes,  $D_{vib}^{(s)}(\omega)$  and  $D_{vib}^{(u)}(\lambda)$ , associated with the INMs of real frequencies  $\omega_\alpha$  and imaginary frequencies  $\omega_\alpha = i\lambda_\alpha$  respectively. The normalization of  $D_{vib}(\omega)$  yields a unit area under the curves of  $D_{vib}^{(s)}(\omega)$  and  $D_{vib}^{(u)}(\lambda)$ , which are usually plotted in the positive and negative axes of  $\omega$ , respectively [10,11].

In the literatures, with the INM eigenvector, the projection operator of particle  $j$  is defined as [18,20]

$$P_j^\alpha = |\vec{e}_j^\alpha|^2 = \sum_{\mu=x,y,z} e_{j\mu}^\alpha \cdot e_{j\mu}^\alpha.$$

In terms of the projection operator, the contribution of particle  $j$  to the vibrational DOS is expressed as

$$D_j(\omega) = \frac{1}{3N-6} \left\langle \sum_{\alpha=1}^{3N-6} P_j^\alpha \delta(\omega - \omega_\alpha) \right\rangle.$$

The integration of  $D_j(\omega)$  over frequency is given as

$$I_j \equiv \int_0^\infty D_j^{(s)}(\omega) d\omega + \int_0^\infty D_j^{(u)}(\lambda) d\lambda = \frac{1}{3N-6} \left\langle \sum_{\alpha=1}^{3N-6} P_j^\alpha \right\rangle.$$

Thus,  $I_j$  is also realized as an ensemble average of all vibrational projection operators associated with particle  $j$ . According to the results given in the following section, we emphasize that the temperature variations of all  $I_j$  quantities of a species in a cluster shed light on the melting behaviour of the cluster.

### 3. Simulation and Melting Behaviour for $\text{Ag}_{17}\text{Cu}_2$

With the Gupta potentials of Cu-Cu, Ag-Ag and Cu-Ag, we generate the configurations of  $\text{Ag}_{17}\text{Cu}_2$  by Brownian-type isothermal MD simulations with a time step of 1 fs [11]. We start the simulation at  $T=0$  and, then, heat up to 1500 K with a step of 10 K. Following a previous work [5], the specific heat of the cluster is calculated by

$$C_V = \frac{\langle E_{tot}^2 \rangle_t - \langle E_{tot} \rangle_t^2}{k_B T^2},$$

where  $E_{tot}$  includes the kinetic energies of all atoms and the Gupta potential energies of every atomic pairs. At each  $T$ , the variation of  $E_{tot}$  is averaged over a long period in a range of  $(1-3) \times 10^{-7}$  s.

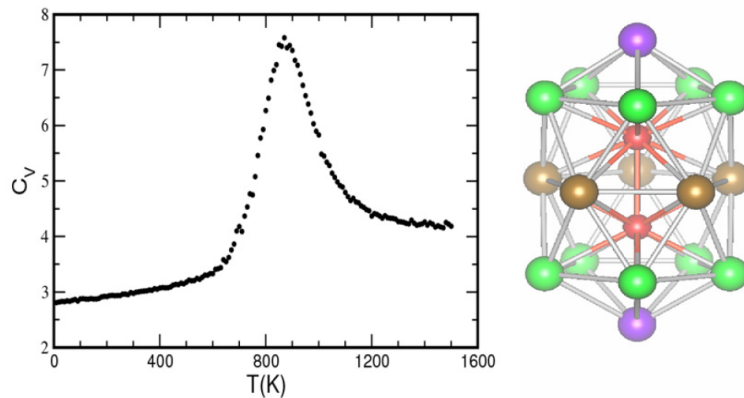


**Figure 1.** Specific heat  $C_V$  (left) and ground-state structure (right) of  $\text{Ag}_{17}\text{Cu}_2$ .  $C_V$  is in unit of  $k_B$ . The atoms in the ground-state structure are classified into four subsets, denoted as  $\text{Cu}^{(2)}$  (red),  $\text{Ag}^{(2)}$  (violet),  $\text{Ag}^{(5)}$  (brown) and  $\text{Ag}^{(10)}$  (green), as in Ref. [11].

In the left part of Fig. 1, the specific heat of  $\text{Ag}_{17}\text{Cu}_2$  shows a maximum located at  $T_m \approx 890$  K. Shown in the right part of Fig. 1 is the ground-state structure of  $\text{Ag}_{17}\text{Cu}_2$  (at  $T=0$ ), which has the  $D_{5h}$  symmetry [21] with the principal axis going through the two centrally located Cu atoms: a five-fold rotational symmetry about the principal axis, a reflection symmetry about the plane containing the middle pentagonal ring and another reflection symmetry about the plane containing the principal axis and anyone of Ag atoms residing in the middle pentagonal ring. Owing to the  $D_{5h}$  point group, we classify the atoms in the ground-state structure presented in Fig. 1 into four subsets of atoms: two Cu atoms, top and bottom Ag atoms, five Ag atoms in the middle pentagonal ring and ten Ag atoms in the upper and lower pentagonal rings, which are denoted as  $\text{Cu}^{(2)}$ ,  $\text{Ag}^{(2)}$ ,  $\text{Ag}^{(5)}$  and  $\text{Ag}^{(10)}$ , respectively [11].

Averaged over  $10^6$  cluster configurations at each temperature, the INM DOS of  $\text{Ag}_{17}\text{Cu}_2$  are depicted in Fig. 2. After removing the contributions of the rotational INMs, which are selected by anyone of the two methods described above, the vibrational INM DOS is obtained. Since the vibrational INM DOS obtained by the two methods are found to be only slight different [11], we only present in this proceedings the results by *Method II*. At  $T=100\text{K}$ , the INM spectra with and without the rotational contributions exhibit structural characteristics and all vibrational INMs possess real frequencies, displaying a solid-like behaviour, since the cluster configurations are around the ground-state structure corresponding to the lowest energy of the potential energy landscape. At  $T=500\text{K}$ , the INM spectra are generally smoothed out and the amount of the imaginary-frequency vibrational INMs are noticeable, which suggests that the cluster has the possibility to surmount the energy barriers to higher-energy excited states. As  $T$  increases further to  $900\text{K}$  or  $1300\text{K}$ , the INM DOS exhibits a large portion of imaginary-frequency vibrational INMs, indicating a liquid-like behaviour, in which a cluster at sufficiently high temperatures would go around everywhere the potential energy landscape.

The INM analysis is applied to the  $\text{Ag}_{17}\text{Cu}_2$  cluster configurations at finite temperatures and at the ground-state structure ( $T=0$ ). At finite  $T$ , the atoms in  $\text{Ag}_{17}\text{Cu}_2$  are also classified into four subsets according to the following procedure: By tracing the atom labels of the subsets in the ground-state structure, the subsets of atoms at a finite temperature can be obtained in a simulation, in which the cluster temperature is gradually raised from zero. At low temperatures, one can recognize the four subsets of atoms by the cluster structures, in which the relative positions of atoms are similar as those in the ground-state structure. On the contrary, at temperatures where the cluster is realized as the liquid-like behaviour, the atom positions of the same species become completely random within the range of cluster size so that the subsets of atoms of  $\text{Ag}^{(2)}$ ,  $\text{Ag}^{(5)}$  and  $\text{Ag}^{(10)}$  lose the identities they had at  $T=0$ . As a result, atoms in the cluster at high temperatures are only distinguished by species of different masses.

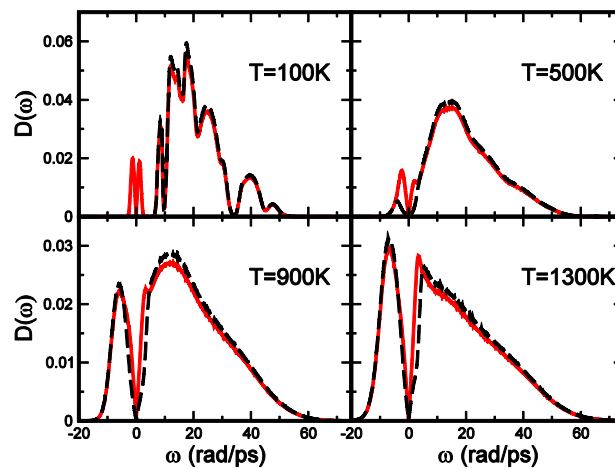


**Figure 2.** Normalized INM DOS of  $\text{Ag}_{17}\text{Cu}_2$  at four temperatures. The red-solid lines are the spectra with the contributions of rotational and vibrational INMs and the black-dashed lines are the spectra by removing the contributions of the rotational INMs selected by *Method II* described in Ref. [11].

Because the atoms in a subset play the same role in dynamics, we average their  $D_j(\omega)$  given as

$$D_X(\omega) = \frac{1}{N_X} \sum_{j=1}^{N_X} D_j(\omega),$$

where the subscript  $X=\text{Cu}^{(2)}, \text{Ag}^{(2)}, \text{Ag}^{(5)}$  and  $\text{Ag}^{(10)}$  and  $N_X$  is the total number of atoms in subset  $X$  [11]. Therefore,  $D_X(\omega)$  is the averaged contribution of an atom in subset  $X$  to all vibrational INMs with  $\omega$ . Shown in Fig. 3 are  $D_X(\omega)$  for the four subsets of atoms of  $\text{Ag}_{17}\text{Cu}_2$  at  $T=0, 100$  and  $500\text{K}$ . At zero temperature,  $D_X(\omega)$  is a bunch of straight lines and, for any subset of atoms, there is no line falling in the range between 30 and 37 rap/ps. The vibrational INMs with  $\omega$  above 37 rap/ps are dominated by the Cu atoms and the INMs with  $\omega$  below 30 rap/ps are dominated by the Ag atoms. At  $T=100\text{K}$ , the temperature effect smears the straight line of  $D_X(\omega)$  at  $T=0$  into a continuous function and the vibrational-frequency gap between 30 and 37 rap/ps is generally filled out. At  $T=500\text{K}$ , with the appearance of the imaginary-frequency lobe,  $D_X(\omega)$  of the three subsets of Ag atoms become similar in spectral shape but are distinguishable from that of the subset  $\text{Cu}^{(2)}$ .

#### 4. Order Parameter by the INM Analysis

By integrating  $D_j(\omega)$  of the vibrational INMs obtained by *Method II* [11], the  $I_j$  values of atoms in the four subsets of  $\text{Ag}_{17}\text{Cu}_2$  are plotted in Fig. 4(a) with a temperature resolution of  $10\text{K}$ . Due to the difference in masses of the Ag and Cu atoms, the  $I_j$  of the Cu atoms are well separated from those of the Ag atoms at all  $T$ . Below  $450\text{K}$ , the  $I_j$  of the three subsets of Ag atoms split into three branches and as  $T$  approaches to zero the three  $I_j$  branches converge to the values corresponding to the subsets of Ag atoms in the ground-state structure. The three branches indicate that the atoms in the cluster in this temperature range vibrate with small amplitudes around the ground-state structure and the vibrations result in a mild increase of the specific heat with temperature. From  $450$  to  $600\text{K}$ , the three  $I_j$  branches are still visibly separated but somewhat defile by exchanges between two branches, physically corresponding to the site permutations among Ag atoms in different subsets or scatter due to the cluster in the excited states. In this temperature range, the cluster structures mostly remain similar as the ground-state configuration but, with some probability, the cluster is driven into the configurations of the first and

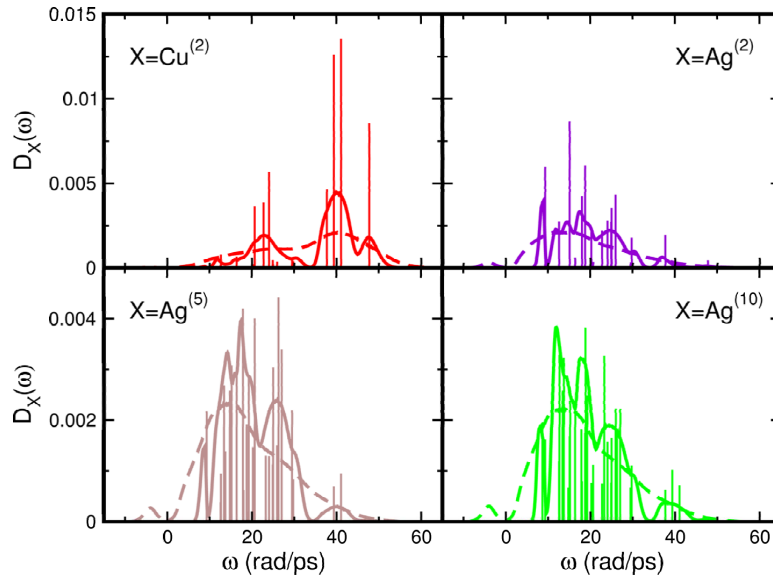


**Figure 3.** Vibrational  $D_X(\omega)$  spectra for the four subsets of atoms of  $\text{Ag}_{17}\text{Cu}_2$ . As in Ref. [11], the straight lines and the solid curves are for the cluster at the ground-state structure and  $100\text{K}$ , respectively. The dashed curves are for the cluster at  $T=500\text{K}$ .

second lowest excited states by thermal activation over the energy barriers in the potential energy landscape [11]. This thermal activation causes the behavior of the specific heat with increasing temperature different from that at low temperatures. Between 600 and 900K, the  $I_j$  of the three subsets of Ag atoms start to coalesce and the branches are no longer distinguishable, indicating that the ground-state structure is being melted and the original subsets of Ag atoms gradually lose their identities. With enough thermal energy, the cluster surmounts energy barriers with a large probability into even higher excited states [11], which are far from the ground state in the configuration space, so that the  $C_V$  within this temperature range increases dramatically and reaches a maximum at  $T=900\text{K}$ . After 900K, the  $I_j$  values of all Ag atoms merge into one, indicating that the ground-state structure could have melted and the Ag atoms are completely random. Corresponding to a sharp drop in the  $C_V$  within this range, the randomness among the Ag atoms is no longer enhanced by increasing further the cluster temperature so that we can safely say that the  $\text{Ag}_{17}\text{Cu}_2$  cluster is in the liquid-like behaviour.

In terms of the  $I_j$  values of the Ag atoms, we propose a new order parameter  $\tau(T)$  for describing the melting transition of  $\text{Ag}_{17}\text{Cu}_2$ . The variation of the  $I_j$  values for the 17 Ag atoms is calculated as

$$\sigma_I^2(T) = \frac{1}{N_{\text{Ag}}} \sum_{j=1}^{N_{\text{Ag}}} I_j^2 - \left( \frac{1}{N_{\text{Ag}}} \sum_{j=1}^{N_{\text{Ag}}} I_j \right)^2,$$

where  $N_{\text{Ag}}=17$ . The order parameter  $\tau(T)$  is defined as the standard deviation  $\sigma_I(T)$  normalized with  $\sigma_I(T=0)$ , i.e.

$$\tau(T) = \frac{\sigma_I(T)}{\sigma_I(T=0)}.$$

The results of  $\tau(T)$  calculated for  $\text{Ag}_{17}\text{Cu}_2$  are shown in Fig. 4(b). Below 300K,  $\tau(T)$  is almost one, signaling that the ground-state structure is well preserved. From 300 to 600K,  $\tau(T)$  declines from one to 0.85, indicating again that the ground-state structure is generally maintained.  $\tau(T)$  starts to drop sharply around  $T=600\text{K}$  and approaches asymptotically to a small value around 890K, which is  $T_m$  defined by the peak position in the  $C_V$  curve shown in Fig. 1. This sharp decay in  $\tau(T)$  marks a melting shake-up of the ground-state structure, with the cluster being thermally activated into the higher-energy excited states. Beyond  $T_m$ ,  $\tau(T)$  stays at a non-zero constant, which is due to the finite size of the cluster. Physically, the constancy in  $\tau(T)$  manifests no further distinction in the atomic distribution under an ensemble average among the Ag atoms by further increasing temperature of the cluster.

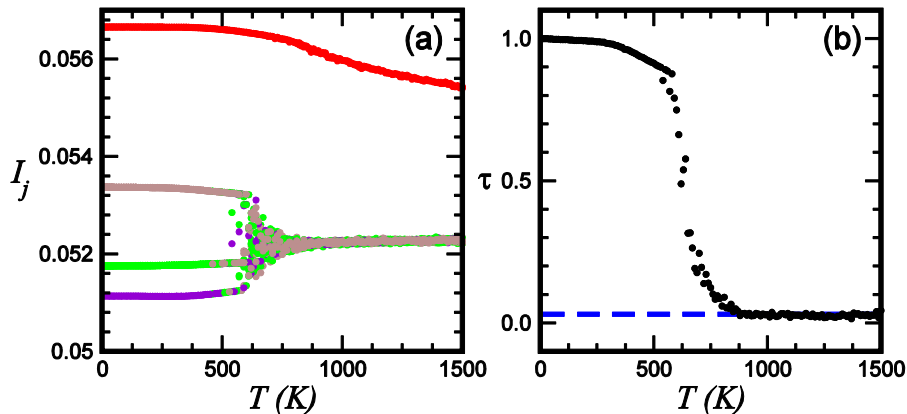


**Figure 4.** (a) Temperature variations of  $I_j$  for the four subsets of atoms (b) Order parameter  $\tau(T)$  vs  $T$ . The dash line is the high-temperature asymptote of  $\tau(T)$ . The figures are referred from Ref. [11].

## 5. Conclusions

We have performed isothermal Brownian-type MD simulations with the Gupta potentials for  $\text{Ag}_{17}\text{Cu}_2$  cluster. With the simulations, the melting behavior of the cluster is obtained by the specific heat data. On the other hand, the dynamic properties of  $\text{Ag}_{17}\text{Cu}_2$  are analyzed by the INM approach. With the projection operators defined by the INM eigenvectors, the vibrational INM DOS,  $D_j(\omega)$ , of each atom is given. With the integral value  $I_j$  of  $D_j(\omega)$  over frequency, we define a new order parameter  $\tau(T)$  as the normalized standard deviation of the  $I_j$  value for the Ag atoms to describe the melting behavior of  $\text{Ag}_{17}\text{Cu}_2$ . In terms of  $\tau(T)$ , the melting behavior of the cluster is distinguished into three temperature regimes: (I) At low temperatures, where  $\tau(T)$  is almost or close to one, the ground-state structure is generally preserved; (II) At intermediate temperatures, where  $\tau(T)$  drops sharply from one to a non-zero small value, the cluster is generally found in the ground-state structure but, with some probability, in the higher-energy excited states; (III) At high temperatures, where  $\tau(T)$  stays at a non-zero value, the cluster rarely resides in the ground-state structure and is almost found in the higher-energy excited states, which are significantly deviated from the ground state in the configuration space. According to our results for the  $\text{Ag}_{17}\text{Cu}_2$  cluster, the three regimes characterized by  $\tau(T)$  are consistent with the melting behavior obtained by the temperature variation of the specific heat. More recently, we have examined the new order parameter for  $\text{Ag}_{14}$  cluster, which specific heat shows both a main peak and a pre-peak at a lower temperature, and the order parameter also works well for  $\text{Ag}_{14}$  cluster [22].

## Acknowledgement

TMW acknowledge supports from National Science Council, Taiwan under Grant No. NSC 101-2112-M-009-007.

## References

- [1] Wales D J 2003 *Energy Landscapes, With Applications to Clusters, Biomolecules and Glasses* (Cambridge University Press, Cambridge)
- [2] Berry R S and Wales D J 1989 *Phys. Rev. Lett.* **63** 1156
- [3] Schmidt M, Kusche R, Kronmüller W, von Issendorff B and Haberland H 1997 *Phys. Rev. Lett.* **79** 99
- [4] Schmidt M, Kusche R, von Issendorff B and Haberland H 1998 *Nature* **393** 238
- [5] Yen T W, Lai S K, Jakse N and Bretonnet J L 2007 *Phys. Rev. B* **75** 165420
- [6] Jellinek J, Beck T L and Berry R S 1986 *J. Chem. Phys.* **84** 2783
- [7] Lynden-Bell R M and Wales D J 1994 *J. Chem. Phys.* **101** 1460
- [8] Doye J P K and Wales D J 1995 *J. Chem. Phys.* **102** 9673
- [9] Calvo F and Spiegelmann F 2000 *J. Chem. Phys.* **112** 2888
- [10] Hsu P J, Luo J S, Lai S K, Wax J F and Bretonnet J L 2008 *J. Chem. Phys.* **129** 194302
- [11] Tang P H, Wu T M, Yen T W, Lai S K and Hsu P J 2011 *J. Chem. Phys.* **135** 094302
- [12] Stratt R M 1995 *Acc. Chem. Res.* **28** 201
- [13] Keyes T 1997 *J. Phys. Chem. A* **101** 2921
- [14] Stanley H E, Buldyrev S V, Giovambattista N, La Nave E, Mossa S, Scala A, Sciortino F, Starr F W and Yamada M 2003 *J. Stat. Phys.* **110** 1039
- [15] Adams J E and Stratt R M 1990 *J. Chem. Phys.* **93** 1332
- [16] Adams J E and Stratt R M 1990 *J. Chem. Phys.* **93** 1358
- [17] Adams J E and Stratt R M 1990 *J. Chem. Phys.* **93** 1632
- [18] Larsen R E, Goodyear G and Stratt R M 1996 *J. Chem. Phys.* **104** 2987
- [19] Page M and McIver Jr. J W 1988 *J. Chem. Phys.* **88** 922
- [20] Buchner M, Ladanyi B M and Stratt R M 1992 *J. Chem. Phys.* **97**, 8522
- [21] Carter R L 1998 *Molecular Symmetry and Group Theory* (Wiley, New York)
- [22] Tang P H, Wu T M, Hsu P J and Lai S K 2012 *J. Chem. Phys.* **137** 244304